Research Square

Preprints are preliminary reports that have not undergone peer review.
They should not be considered conclusive, used to inform clinical practice,
or referenced by the media as validated information.

Effect of Maturity on the Physicochemical and Functional Properties of Euryale Ferox Flour and Starch

Juan Chen[1]
Anhui University
Yamei Lu[1]
Anhui University
Yue Huo[2]
Chuzhou University
Yang Liu[2]
Chuzhou University
Cuan Zhang[2]※
zhangcuan2005@126.com
Chuzhou University

Research Article

Keywords: maturity, Euryale ferox flour, Euryale ferox starch, physicochemical and functional properties

Posted Date: September 12th, 2025

DOI: https://doi.org/10.21203/rs.3.rs-7476371/v1

License: This work is licensed under a Creative Commons Attribution 4.0 International License.
Read Full License

Additional Declarations: No competing interests reported.

Abstract

Euryale ferox seeds can be classified into three types: tender, green, and old seeds based on their growth period. This study aimed to compare the physicochemical and functional properties of *Euryale ferox* flour and starch samples at varying stages of maturity. These samples were characterized by the methods of scanning electron microscope, X-ray diffraction, rapid viscosity analysis, Fourier transform infrared spectroscopy and rheological measurements, and the nutritional composition, microstructure, crystalline characteristics, pasting behavior, molecular structure, and rheological properties of both whole flour and starch were analyzed in the article. Results showed that starch contents raised significantly with increasing maturity, while amylose-to-amylopectin ratio decreased. Relative crystallinity and pasting viscosities also increased. Scanning electron microscope revealed polygonal starch granules, and its edges becoming sharper with maturity. Rheological tests indicated that both G' and G" of EF and ES samples increased significantly with increasing maturity. These findings suggest that seed maturity has a significant impact on starch structure and functionality. The importance of selecting suitable mature raw materials in the processing of *Euryale ferox* products was emphasized.

Introduction

Euryale ferox is the kernel of *Euryale ferox* Salisb (Nymphaeales), which is a traditional Chinese herb and functional food material. Modern pharmacological studies have shown that *Euryale ferox* has beneficial functions such as antioxidant[1], hypoglycemic[2], and anti-cancer[3] effects. *Euryale ferox* is rich in starch (77.5–78.1%) and protein (9.96%) [4], with a negligible lipid content, so it is a typical starch-based food material. In its processing, *Euryale ferox* seeds are usually categorized into three types: tender seed (TS), green seed (GS) and old seed (OS) based on their developmental stage and texture. TS is characterized by non-lignified shell that can be manually peelable; GS has shell that begin to lignify and can be gently cracked with teeth; OS is fully mature with completely lignified and hard shell.

According to the previous research [5], significant variations exist in the starch, protein, and amylose/amylopectin content of *Euryale ferox* kernels at different maturities. Among them, the total starch content increases with maturity, reaching the highest at 25 days after flowering, while the reducing sugar content decreases. Similar phenomena have been observed in other crops, such as *lotus* seeds and *sorghum*. Sun et al. [6] found that with increasing maturity, the particle size, crystallinity, and amylose content of lotus seed starch significantly increased. Studies have shown that *Sorghum* samples of amylose ranged from 16.3% in 10 days to 23.3% amylose in 35 days, and starch thermal properties were also altered due to maturity, most notably the gelatinization enthalpy (ΔH) was 16.1 J/g at 14 days, 11.95 J/g at 35 days, and 9.45 J/g at 56 days [7].These findings in related crops suggest that maturity is a critical factor regulating starch properties, however, there is limited understanding of the changes in the physicochemical and functional properties of *Euryale ferox* flour and starch throughout seed development.

This study aims to utilize *Euryale ferox* seeds of varying maturities as raw materials, employing physicochemical analysis in conjunction with advanced characterization techniques to investigate the differences in physicochemical and functional properties of *Euryale ferox* at different maturities. This research seeks to provide a theoretical foundation for the quality evaluation and advanced processing of *Euryale ferox* products.

Materials and methods

Reagents

Anhydrous ethanol, 3,5-dinitrosalicylic acid, hydrochloric acid, propylene glycol, sodium hydroxide, etc., all of which are analytical grade reagents, were purchased from Sinopharm Chemical Reagent Co., Ltd. Amylose standard (purity > 98%) and amylopectin standard (purity > 98%) were purchased from Shanghai Chemical Reagent Co., Ltd. Neutral protease (200,000 u/g) was purchased from Nanning Pang Bo Biological Engineering Co., Ltd.

Materials

Fresh *Euryale ferox* seeds at varying stages of maturity, including TS, GS, and OS, were collected from the *Euryale ferox* planting base in Dingyuan County, Chuzhou City, Anhui Province, China, in 2023.

Preparation of Euryale ferox flour (EF)

Euryale ferox seeds were thoroughly cleaned and dried for 12 h at 40 ∘C in a hot air oven (BPG-9140A, Shanghai Yiheng Scientific Instruments Co., Ltd.). The shell was manually removed, the kernel was taken out, and put into a grinder (L10-C051, Jiu yang Co., Ltd, China) and sieved through a 100-mesh sieve to obtain *Euryale* flour (EF). The EF samples were stored in self-sealing bags for later use.

Preparation of Euryale ferox starch (ES)

ES samples were prepared according to the method reported by Zhang et al. [8]. Using EF with vary maturity as the raw material, water was added to prepare a 14% suspension, and then 1.4% neutral protease was added for low-temperature enzymatic hydrolysis (40°C, 5.5 h). After enzymatic hydrolysis, the supernatant was obtained by low-speed centrifuging (400 rpm, 5 min). (TDZ5-WS, Hunan Xiangyi Laboratory Instrument Development Co., Ltd., China). The precipitate was added with 10–20 times the volume of water, and using a high-pressure homogenizer (FA25, Gongyi Yuhua Instrument Co., Ltd., China), high-speed homogenization for 3–5 min, and centrifuged again at low speed. The supernatants obtained from centrifugation were combined. The precipitate was collected after centrifuging at 4000 rpm for 10 min (GL-21M, Hunan Xiangyi Laboratory Instrument Development Co., Ltd., China). After drying in an oven at 40°C, the ES sample was finally crushed and sieved through a 100-mesh sieve. The ES samples were stored in self-sealing bags for later use.

Determination of nutritional components

Moisture content was determined according to ISO 712:2009 (Cereals and cereal products–Determination of moisture content–Reference method) using a precision forced air oven (BPG-9140A, Shanghai Yiheng Scientific Instruments Co., Ltd., China) maintained at 105 ℃ until constant weight.

Crude protein content was determined according to ISO 20483:2013 (Cereals and pulses–Determination of the nitrogen content and calculation of the crude protein content–Kjeldahl method) using an automatic Kjeldahl Nitrogen Analyzer (K1100, Jinan Hanon Instruments Co., Ltd., China). The nitrogen content was converted to crude protein using a factor of 6.25.

Ash content was determined according to ISO 2171:2007 (Cereals, pulses and by-products–Determination of ash yield by incineration) using a muffle furnace (BA-4-104, Shanghai Benang Scientific Instruments Co., Ltd., China) at 550 ℃ for 12 h (until white ash was obtained).

Starch content was determined according to ISO 6493:2000 (Animal feeding stuffs–Determination of starch content – Polarimetric method), with modifications: starch-iodine complex absorbance was measured instead of polarimetry. Starch was hydrolyzed with HCl (0.5 M, 100°C, 30 min), The starch-iodine complex absorbance was measured at 540 nm using a UV-Vis spectrophotometer (UV-1900i, Shimadzu, Japan).

Amylose content was determined according to ISO 6647-2: 2020 (Rice Determination of amylose content–Part 2: Routine methods) using an iodine colorimetric assay at 720 nm.

Scanning electron microscopy (SEM)

The SEM of EF and ES samples was determined following the method of Lv et al. [9] with modifications. A small amount of sample powder was evenly sprinkled on the conductive adhesive, sputtered with gold for about 10 seconds, and the unadhered samples were blown off with an ear wash bulb. A field emission scanning electron micro-scope (SU8010, Hitachi High-Technologies Corporation, Japan) equipped with a HORIBA X-max N energy dispersive spectrometer was used for testing in secondary electron mode, with an accelerating voltage of 5 kV. The magnification was 1000 times for EF and 10000 times for ES.

X-ray diffraction (XRD)

The XRD of EF and ES samples were determined according to the method described by Zhan et al. [10] with minor modifications. Samples were equilibrated at room temperature for 24 hours. Then, it was analyzed with slight modifications using an XRD instrument (D8-Advance, Bruker Technology Co., Ltd., China). The voltage was set to 30 kV, the scanning rate was 12 °/min, and the scanning range was 5 °-40 °. Origin software was used to calculate the relative crystallinity (RC) of the samples.

Rapid viscosity analysis (RVA)

The RVA properties of EF and ES samples were determined based on the method of Niu et al. [11] with minor modifications. Use a RVA instrument (Tec Master, Swedish Perten Instruments, Sweden), Put 3.0 g of sample (dry basis) into an aluminum sample box, mixed with 25 ml of deionized water to prepare a suspension, and tested in an RVA instrument. The determination procedure was as follows: hold at 50°C for 1 min, heat from 50°C to 95°C at a rate of 3.75°C/min, hold at 95°C for 2.5 min, and cool from 95°C to 50°C at a stirring rate of 160 r/min.

Differential scanning calorimetry (DSC)

The DSC method was used to determine the thermal stability of EF and ES samples according to Man et al. [12]. 3 mg of starch was mixed with 9 μL of ultrapure water, sealed in an aluminum pan, and stored at 4°C overnight to allow sufficient water absorption of the starch. After equilibrating at room temperature for 1 hour, the samples were analyzed using a differential calorimetric scanner (NETZSCH 3500, NETZSCH-Gerätebau GmbH, Germany). at a rate of 10°C/min within the temperature range of 25–130°C to determine the thermodynamic characteristic parameters of starch, including gelatinization onset temperature (To), peak temperature (Tp), conclusion temperature (Tc), and gelatinization enthalpy (ΔH).

Fourier transform infrared spectroscopy (FTIR)

The FTIR of EF and ES samples was determined based on the method of Wang et al. [13]. 1 mg of dried sample was thoroughly mixed with 100 mg of potassium bromide powder in a mortar and pressed into tablets. A Fourier transform infrared spectrometer (IRAffinity-1S, Shimadzu Manufacturing Co., Ltd., Japan) was used for scanning in the wavenumber range of 400–4000 cm^{-1} with a resolution of 8 cm^{-1}. The obtained spectrograms were subjected to smoothing and baseline correction. The spectra within 1200 – 800 cm^{-1} were deconvoluted with a resolution enhancement factor of 1.9, a half-peak width of 26 cm^{-1}, and a noise target of 2.4. The peak intensities at 1022 and 1047 cm^{-1} were determined, and the ratio of peak intensities at 1047 cm^{-1} to 1022 cm^{-1} ($R_{1047/1022}$) was calculated to represent the short-range order of starch samples.

The solubility (S) and swelling power (SP)

The S and SP of EF and ES samples were determined according to the method described by Liu et al. [14], 0.6 g (dry basis) of starch sample (Ws) was placed in a centrifuge tube (with known mass), mixed with 30 ml of distilled water to prepare a starch suspension, and heated and oscillated in a 95°C water bath for 30 min. Then, it was rapidly cooled to room temperature in an ice bath and centrifuged (4000 r/min, 10 min). The supernatant was taken into a pre-weighed aluminum box, dried to constant weight at 95–105°C, and the mass of the dried supernatant (W_1) was recorded and calculated. After

centrifugation, the mass of the remaining precipitate in the centrifuge tube was weighed as W_2. S (formula 1) and SP (formula 2) were calculated as follow equations:

$S\ (\%) = (W_1 / W_S) \times 100$ (1)

$SP\ (g/g) = W_2 / (Ws - W_1)$ (2)

Rheological analysis

The rheological analysis of EF and ES samples was analyzed according to the method described by Irani et al. [15]. The rheological properties of the samples were analyzed with the rheometer (DHR-1, TA Instruments, USA). 100 mg of sample was dispersed in 1 mL of distilled water (magnetically stirred at 900 rpm at room temperature for 1 h to ensure thorough mixing), and then gelatinized in a boiling water bath for 30 min.

Dynamic oscillatory rheological measurement: The starch paste was placed on the stage, using a plate with a diameter of 40 mm and a gap of 1 mm. The temperature was set to 25°C, the stress was 1%, the equilibrium time was 60 s, and the frequency was tested from 0.1 to 10 Hz. Data were collected and analysed, including storage modulus (G'), loss modulus (G"), and loss factor tan δ (G"/G').

Statistical analysis

All experimental measurements were made in triplicate and the experimental results were expressed as mean ± standard deviation. Excel 16 and Origin 2024 was used for plotting. To identify significant differences ($p < 0.05$), results were deter- mined using the Duncan multiplicity method with SPSS 25.0 software.

Results and discussion

Main nutritional components analysis

The main nutritional components of samples are shown in Table 1. The primary nutritional components of EF are starch (77.00%-79.36%) and protein (11.36%-11.46%). With increasing maturity, the contents of starch, polyphenols, and crude fiber significantly increased ($p < 0.05$), while the fat and total protein contents showed no significant difference. However, the soluble protein content significantly decreased. With increasing maturity, the amylose content in EF significantly decreased. Some studies suggest that amylose acts as a precursor for amylopectin synthesis, and a branched structure of amylopectin is formed through the catalysis of the starch branching enzyme (SBE). In other words, amylose is synthesized first and then converted into amylopectin under the action of SBE [16]. A similar trend has been observed in lotus seeds, where the amylose content in immature seeds was 30.14%, whereas it decreased to 20.70% in mature seeds [17]. The amylose content in ES ranged from 36.25–39.15%. This result is consistent with that reported by Yang et al. [18], but it is significantly higher than that of other staple crops, such as rice (17%), wheat flour (24%), and high-amylose corn (26%) [19]. Therefore, the high amylose content may contribute to the characters of easy retrogradation and resistance to digestion of

EF. In ES samples with different maturities, the starch content is 95.58%-96.70%, residual protein is 1.03%-1.09%, and residual ash is 0.07%-0.11%, with no significant differences between samples.

Table 1
Main nutritional components of EF and ES at different maturity levels

Samples	EF			ES		
	TS	GS	OS	TS	GS	OS
Starch /%	77.00 ± 0.36^{f}	78.41 ± 0.25^{e}	79.36 ± 0.23^{d}	95.58 ± 0.26^{c}	96.70 ± 0.33^{a}	96.21 ± 0.40^{b}
Protein /%	11.46 ± 0.10^{a}	11.38 ± 0.07^{a}	11.36 ± 0.07^{a}	1.07 ± 0.08^{b}	1.03 ± 0.07^{b}	1.09 ± 0.08^{b}
Water soluble protein /%	2.34 ± 0.02^{a}	2.01 ± 0.02^{b}	1.97 ± 0.05^{c}	ND	ND	ND
Crush fiber /%	1.34 ± 0.02^{a}	1.57 ± 0.03^{b}	1.70 ± 0.07^{c}	ND	ND	ND
Total phenol /%	1.41 ± 0.02^{c}	1.55 ± 0.05^{b}	1.76 ± 0.07^{a}	0.75 ± 0.08^{d}	0.68 ± 0.07^{d}	0.70 ± 0.08^{d}
Fat /%	0.31 ± 0.03^{a}	0.35 ± 0.05^{a}	0.38 ± 0.04^{a}	ND	ND	ND
Ash /%	0.96 ± 0.05^{b}	1.17 ± 0.07^{b}	1.31 ± 0.06^{a}	0.17 ± 0.015^{c}	0.18 ± 0.015^{c}	0.19 ± 0.015^{c}
Amylose /%	39.87 ± 0.10^{a}	38.95 ± 0.18^{c}	36.89 ± 0.15^{e}	39.15 ± 0.13^{b}	38.55 ± 0.13^{d}	36.25 ± 0.12^{f}

EF *Euryale ferox* flour, ES *Euryale ferox* starch, TS tender seeds, GS green seeds, OS old seeds, ND non-detected. Data are expressed as mean (n = 3) ± standard deviation (SD). The different letters in each analysis represent significant differences ($p < 0.05$).

XRD analysis

The result of XRD is a useful method to assess and quantify long-range crystallization order in starch sample [20]. As shown in Fig. 1, both EF and ES with different maturities exhibited diffraction peaks at 15.2°、17.0°、18.3°、and 23.6°, which are characteristic of A-type crystals, consistent with previous reports by Wang et al. [21]. The RC values of EF samples (TS, GS, and OS) significantly increased with increasing maturity, reaching 33.10%, 35.21%, and 36.70% respectively. The RC values of ES prepared by low-temperature enzymatic hydrolysis also showed a similar trend. Jiang et al. [22]found that the RC values of starch show an opposite changing trend to the amylose content, indicating that the orderly arranged amylopectin in starch granules is the key source of its crystallinity. Compared to EF samples, ES samples exhibited higher RC values, which can be attributed to their higher starch contents (Table 1).

SEM analysis

As shown in Fig. 2, EF exhibits numerous spherical starch aggregates, which are tightly bound by starch granules and proteins, with diameters ranging from 10 to 50 μm. In the ES sample, there are only starch granules with a particle size of 1–5 μ m, and there is no spherical aggregate structure. These observations suggest that ordinary crushing method is difficult to completely destroy the aggregate structure in EF, and such aggregate structure will inevitably influence the gelatinization, aging, and digestion characteristics of starch. There is no significant difference in morphology among the three EF samples with different maturity levels, and the size and quantity of starch granules have changed, but their overall structure remains relatively stable (Fig. 2a, b, c). However, there are certain differences in the microstructure of the three different maturity ES samples, such as the smooth edges of starch particles in tender seeds, which are not as sharp as those in old seeds (Fig. 2d, e, f). It is speculated that in the endosperm of tender seeds, the squeezing effect between particles is weak. As maturity increases, due to the increase in starch particle size and quantity, starch particles squeeze each other, and the edges of the particles gradually become sharper. Wu et al. [5]also found that at 10 days after flowering, the starch bodies and granules in the endosperm of the *Euryale ferox* were smaller and arranged more loosely.

Pasting properties and thermal stability analysis

The pasting properties of samples are shown Fig. 3 and Table 2. The results showed that maturity significantly influences the gelatinization characteristics of EF and ES samples. With increasing maturity, the onset pasting temperature and peak time of EF samples significantly increased, whereas peak viscosity, trough viscosity, and final viscosity exhibited a significant decreasing trend ($p < 0.05$). This suggests that EF with lower maturity is more readily gelatinized. These findings are supported by SEM images in Fig. 2, which indicate that in TS and GS samples, the binding between starch granules is relatively loose within the spherical aggregate structure, making it easier for water to enter and cause gelatinization [23]. Similar trends have been reported in the development of wheat and rice seeds [24]. In addition, This result may also be related to the crystallinity of the sample. For instance, the OS flour with the highest crystallinity has the lowest viscosity, and its RVA curve does not have obvious peak viscosity and trough vicosity, which is significantly different from the RVA profiles of TS and GS flours (Fig. 3c). The RVA analysis results of three different maturity levels of ES revealed that with increasing maturity, there was no significant change in the onset temperature and peak time, but peak viscosity, trough viscosity, and final viscosity all showed a significant decreasing trend ($p < 0.05$). The reason may be related to the increase in relative crystallinity of starch samples (Fig. 1), as the old seed starch with the highest crystallinity is more difficult to gelatinize.

As shown in Fig. 4 and Table 2, with increasing maturity, the onset gelatinization temperature (To), peak temperature (Tp), conclusion temperature (Tc), and enthalpy change (ΔH) of EF and ES samples showed a significant increasing trend ($p < 0.05$). Based on the trend of changes in amylose content in Table 1, it is speculated that the amylopectin content in samples increases with increasing maturity, which can maintain a more ordered and stable crystal structure of starch granules and thus have stronger

resistance to the gelatinization process[25]. The thermodynamic properties of starch to some extent reflect the compactness of starch crystallization. The distribution of branched starch chain length, the proportion of various components in starch, and changes in fine structure during different stages of development can all affect the temperature of gelatinization[29]. The enthalpy change during gelatinization mainly reflects the loss of the double helix sequence in starch molecules [26]. Cooke et al. [27] found that the enthalpy of gelatinization decreases with the increase of amylose content, which is consistent with the results of this experiment.

Table 2 Pasting properties of EF and ES samples at different maturity levels

		EF			ES		
		TS	GS	OS	TS	GS	OS
RVA	Pasting time / ℃	78.40 ± 0.98c	79.10 ± 0.45d	84.90 ± 0.34^{a}	81.70 ± 0.25^{b}	80.10 ± 0.40^{b}	81.60 ± 0.36^{b}
	Peak viscosity /cp	3624 ± 45.89^{d}	2316 ± 34.08^{f}	965 ± 44.09^{g}	6208 ± 45.09^{a}	5664 ± 46.40^{b}	5112 ± 34.98^{c}
	Trough /cp	2998 ± 23.89^{c}	2079 ± 25.09^{d}	846 ± 19.09^{e}	4172 ± 45.90^{a}	4011 ± 34.00^{a}	3403 ± 30.34^{b}
	Breakdown /cp	626 ± 15.89^{c}	237 ± 13.78^{d}	119 ± 10.98^{e}	2036 ± 21.09^{a}	1653 ± 34.90^{b}	1709 ± 20.98^{b}
	Final viscosity /cp	5255 ± 45.09^{c}	3697 ± 34.98^{d}	2610 ± 25.98^{e}	6073 ± 30.89^{a}	5615 ± 35.80^{b}	5094 ± 40.98^{c}
	Setback /cp	2257 ± 23.45^{a}	1618 ± 20.98^{d}	1764 ± 17.98^{c}	1901 ± 18.78^{b}	1691 ± 15.60^{d}	1604 ± 18.90^{d}
	Peak time /min	5.5 ± 0.15^{b}	5.9 ± 0.20^{b}	7.0 ± 0.35^{a}	5.0 ± 0.14^{b}	5.0 ± 0.23^{b}	5.4 ± 0.23^{b}
DSC	To /℃	72.08 ± 0.22^{d}	72.94 ± 0.32^{c}	75.67 ± 0.35^{a}	70.68 ± 0.33^{f}	72.29 ± 0.35^{e}	74.11 ± 0.36^{b}
	Tp /℃	77.04 ± 0.01^{d}	77.27 ± 0.02^{c}	79.78 ± 0.03^{a}	75.89 ± 0.02^{f}	76.18 ± 0.03^{d}	78.50 ± 0.01^{b}
	Tc /℃	83.39 ± 0.02^{d}	83.91 ± 0.03^{c}	84.46 ± 0.01^{a}	82.30 ± 0.02^{f}	82.65 ± 0.03^{e}	84.33 ± 0.02^{b}
	ΔH /J/g	2.62 ± 0.02^{d}	3.02 ± 0.01^{b}	3.62 ± 0.03^{a}	2.47 ± 0.01^{e}	2.313 ± 0.02^{f}	2.71 ± 0.03^{c}

Data are the mean value ± standard deviation (n = 3). RVA and DSC indicate results obtained by rapid viscosity analysis and differential scanning calorimetry, respectively. EF *Euryale ferox* flour, ES *Euryale*

ferox starch, TS tender seeds, GS green seeds, OS old seeds, To onset temperature, Tp peak temperature, Tc end temperature, ΔH enthalpy change. Values followed by different letters in the same column are significantly different ($p < 0.05$).

Analysis of solubility (S) and swelling power (SP)

As shown in Fig. 4, with increasing maturity, the S value of EF samples showed a significant decrease trend, while the SP value showed a significant increase trend ($p < 0.05$). As the maturity increases, changes such as a decrease in amylose content (Table 1), an increase in starch crystallinity (Fig. 1), a decrease in water-soluble protein content (Table 1), and a denser spherical aggregate structure can all lead to a decrease in the S value of the samples. The SP value is generally associated with the hydration capacity of macromolecules such as starch, cellulose and protein within the gelatinization system [28]. With increasing seed maturity, the interaction between starch granules and protein molecules strengthens, and the content of water-insoluble gluten increases (Table 1), all of which can increase its SP value.

As maturity increases, the S value of ES samples significantly decreases, consistent with the trend of EF samples. This result may be related to the decrease in amylose content in the sample. Among the ES samples, GS had the highest SP value, followed by OS, and TS had the lowest. The study by Ao et al. [29] showed that there was no significant change in the SP of *Euryale ferox*, corn, and wheat, which may be influenced by factors such as climate, plant maturity, and soil.

FTIR analysis

As shown in Fig. 5, no significant differences were observed in the FTIR spectra of varying maturities EF and ES samples. The common peaks of the two types of samples mainly include 3411, 2928, 1655, 1345, 1163, and 1086 cm^{-1}, which correspond to O-H stretching vibration, C-H stretching region, C-H bending vibration, and C-O-C stretching vibration of glucose at 1163 and 1086 cm^{-1}, respectively [30]. It showed that the main nutritional components in EF and ES samples of different maturity levels are basically the same, and no new chemical bonds and functional groups have been found.

The short-range structure of starch can be characterized by absorbance at 1047 cm^{-1} (crystalline region) and 1022 cm^{-1} (amorphous region), and the short-range orderliness of starch can be evaluated based on their ratio ($R_{1047/1022}$) [31]. As shown in Fig. 5, with increase of maturity of *Euryale ferox* seed, the $R_{1047/1022}$ ratio showed a significant increasing trend ($p < 0.05$). Among them, the degree of orderliness of old seeds is the highest, indicating that the short-range orderliness of starch in Euryale seeds increases with seed maturity. Speculation suggests that it is related to the increase in branched starch branches and the decrease in amylose content in OS [20]. In addition, the trend of changes in the RC results of ES samples is completely consistent with its $R_{1045/1022}$ result. This also confirms the above speculation.

Rheological property

Rheological property is one of the important functional properties of food. For gel food containing starch and protein, the storage modulus (G ") and loss modulus (G ") can be measured by frequency scanning of rheometer without damaging the gel structure. The storage modulus (G ') reflects the elastic response of starch gel, that is, the ability to store and rebound energy in dynamic deformation. The loss modulus (G ") characterizes the viscous dissipation ability of starch systems and reflects the energy loss caused by molecular chain breakage or slip [32]. As shown in Fig. 6, with increasing maturity, the G 'and G' 'values of EF and ES samples significantly increase, and the G' value of the same sample is always greater than its G " value. At the same frequency, the G 'and G "values of EF samples significantly increased with increasing maturity ($p < 0.05$). On the one hand, it is due to the synergistic effect between other coexisting components in EF sample and starch, for example, cellulose can enhance the rigidity of gel network through physical filling effect[33]; Protein can be cross-linked with starch through chemical bond, and its mechanism is similar to the enhancement effect of β - glucan in oats on starch gel[34]. On the other hand, as the maturity increases, the starch content increases and the viscosity of the sample increases, which also leads to an increase in its loss modulus (G ") [35]. In addition, at the same frequency, the G 'and G "values of ES samples also significantly increase with increasing maturity. It is speculated that this is related to the increase in RC value of the ES samples (Fig. 1), which means that the more stable the starch crystallization zone, the stronger its shear resistance[36].

Conclusion

Research has shown that the maturity stage of *Euryale ferox* seeds significantly affects the physicochemical and functional properties of both EF and ES. With advancing maturity, the starch and total phenolic contents in EF show a significant increase trend, while the soluble protein content and proportion of amylose show a significant decrease trend ($p < 0.05$). Concurrently, the number of spherical aggregates in EF samples increases, and the RC value of the samples significantly increases. with increasing maturity level, the sample's onset temperature shows an increasing trend, indicating a significant increase in its thermal stability; The S value significantly decreases and the SP value significantly increases; The short-range orderliness, G ', and G " of starch also significantly increased ($p < 0.05$).

Declarations

Conflict of interest:

The authors declare no competing interests.

Funding:

This project was supported by funds from Major Project of Natural Science Research in Anhui Colleges and Universities (KJ2021ZD0134); Chuzhou Science and Technology Mission Team Project (2023tpt08);

Key Project of Chuzhou University (2022XJZD17). We also thank the teachers and classmates for their support.

Author Contribution

J. C.: Writing-original draft, Methodology, Data curation, Conceptualisation. Y. M. L.: Methodology, Investigation, Conceptualisation. Y. H.: Formal analysis. Y.L: Supervising the work. C. Z.: Writing– review & editing, Methodology, Investigation, Conceptualisation.

Data availability:

Data will be made available on request.

References

1. Wu, C. Y., Chen, R., Wang, X. S., Shen, B., Yue, W., & Wu, Q. A. (2013) Antioxidant and Anti-Fatigue Activities of Phenolic Extract from the Seed Coat of Euryale ferox Salisb. and Identification of Three Phenolic Compounds by LC-ESI-MS/MS. Molecules 18(9): 11003-11021. https://doi.org/10.3390/molecules180911003
2. Zhang, W. N., Su, R. N., Gong, L. L., Yang, W. W., Chen, J., Yang, R., Wang, Y., Pan, W. J., Lu, Y. M., & Chen, Y. (2019) Structural characterization and in vitro hypoglycemic activity of a glucan from Euryale ferox Salisb. seeds. Carbohydr. Polym 209: 363-371. https://doi.org/10.1016/j.carbpol.2019.01.044
3. Nam, G. H., Jo, K. J., Park, Y. S., Kawk, H. W., Kim, S. Y., & Kim, Y. M. (2019). In vitro and in vivo Induction of p53-Dependent Apoptosis by Extract of Euryale ferox Salisb in A549 Human Caucasian Lung Carcinoma Cancer Cells Is Mediated Through Akt Signaling Pathway. Front. Oncol *9*: 13406. https://doi.org/10.3389/fonc.2019.00406
4. Kumar, M. M., Goudar, G., Sharma, P., Vishwakarma, R., Gogoi, P., Mahajan, A., Chandragiri, A., Kalpuri, S., Geddam, J. J. B., Suresh, C., Chary, M., Venketrajireddy, G., Radhika, M. S., Sreenu, P., & Tulja, B. (2023) Differentiating the nutrient composition, in-vitro starch digestibility, individual polyphenols and anti-oxidant properties of raw and popped makhana (Euryale ferox). J. Food Meas. Charact 17(6): 5828-5844. https://doi.org/10.1007/s11694-023-02074-5
5. Wu, P., Liu, A. L., Zhu, Y., Li, X., Wang, Y. H., & Li, L. J. (2022) Proteomic analysis of Euryale ferox Salisb seeds at different developmental stages. Gene 834: 146645. https://doi.org/10.1016/j.gene.2022.146645
6. Sun, S. W., Lin, H., Yang, B. K., Zeng, S. X., Lin, S. L., Zheng, B. D., & Guo, Z. B. (2019) □□□□□□□□□□□□□□□□□□□□□□□□□□□□ [Structural properties of starch from fresh lotus seeds of different varieties and maturity stages]. □□□□□□□ (Chinese Journal of Tropical Crops) 40 (09): 1831–1837.

7. Kaufman, R. C., Wilson, J. D., Bean, S. R., Xu, F., & Shi, Y. C. (2017) Sorghum starch properties as affected by growing season, hybrid, and kernel maturity. J. Cereal Sci 74: 127-135. https://doi.org/10.1016/j.jcs.2017.01.014
8. Zhang, C., Liu, Y., Chen, Z. H., Chen, J., & Wu, H. J. (2021) [A synchronous enzymatic processing method for single-grain raw Euryale ferox starch and related products] (Chinese Patent No. CN110372801B). National Intellectual Property Administration, PRC.
9. Lv, X. X., Hong, Y., Gu, Z. B., Cheng, L., Li, Z. F., Li, C. M., & Ban, X. F. (2024) Effect of solution on starch structure: New separation approach of amylopectin fraction from gelatinized native corn starch. Carbohydr. Polym. 329:121770. https://doi.org/10.1016/j.carbpol.2023.121770
10. Zhan, Q., Ye, X. T., Zhang, Y., Kong, X. L., Bao, J. S., Corke, H., & Sui, Z. Q. (2020) Starch granule-associated proteins affect the physicochemical properties of rice starch. Food Hydrocolloids 101: 105504. https://doi.org/10.1016/j.foodhyd.2019.105504
11. Niu, B., Chao, C., Cai, J. J., Yan, Y. Z., Copeland, L., Wang, S., & Wang, S. J. (2019) The effect of NaCl on the formation of starch-lipid complexes. Food Chem 299: 125133. https://doi.org/10.1016/j.foodchem.2019.125133
12. Man, J. M., Lin, L. S., Wang, Z. F., Wang, Y. P., Liu, Q. Q., & Wei, C. X. (2014) Different Structures of Heterogeneous Starch Granules from High-Amylose Rice. Journal of Agricultural and Food Chem 62(46): 11254-11263. https://doi.org/10.1021/jf503999r
13. Wang, B., Gao, W., Kang, X. M., Dong, Y. Q., Liu, P. F., Yan, S. X., Yu, B., Guo, L., Cui, B., & Abd El-Aty, A. M. (2021) Structural changes in corn starch granules treated at different temperatures. Food Hydrocolloids 118: 106760. https://doi.org/10.1016/j.foodhyd.2021.106760
14. Liu, M. Y., Guo, X. X., Ma, X. Y., Xie, Z. R., Wu, Y. W., & Ouyang, J. (2024) Physicochemical properties of a novel chestnut porous starch nanoparticle. Int. J. Biol. Macromol261: 129920. https://doi.org/10.1016/j.ijbiomac.2024.129920
15. Irani, M., Razavi, S. M. A., Abdel-Aal, E. M., Hucl, P., & Patterson, C. A. (2019) Viscoelastic and textural properties of canary seed starch gels in comparison with wheat starch gel. Int. J. Biol. Macromol..124: 270-281. https://doi.org/10.1016/j.ijbiomac.2018.11.216
16. Song, H. Y., Sun, H., Dong, G. Q., Yang, H., Xin, J., Yang, D., Deng, X. B., Liu, J., Su, Y. Y., & Yang, M. (2024) NnSBE1 encodes a starch branching enzyme involved in starch biosynthesis in lotus seeds. Int. J. Biol. Macromol. 279: 135104. https://doi.org/10.1016/j.ijbiomac.2024.135104
17. Sun, Z. X., Chen, J., Dai, T. T., Lv, C. L., Liang, R. H., Liu, W., Liu, C. M., & Deng, L. Z. (2024) Effect of maturity on the drying characteristics of lotus seed and molecular structure, gelation and digestive properties of its starch. Carbohydr. Polym., 345: 122589. https://doi.org/10.1016/j.carbpol.2024.122589
18. Yang, Y. X., Chen, Q., Yu, A. Z., Tong, S., & Gu, Z. Y. (2021) Study on structural characterization, physicochemical properties and digestive properties of euryale ferox resistant starch. Food Chem 359: 129924. https://doi.org/10.1016/j.foodchem.2021.129924

19. Doti, S., Suárez-Belloch, J., Latorre, M. A., Guada, J. A., & Fondevila, M. (2014) Effect of dietary starch source on growth performances, digestibility and quality traits of growing pigs. Livest. Sci 164: 119-127. https://doi.org/10.1016/j.livsci.2014.03.016
20. Li, M. J., Wang, H. R., Tong, L. T., Fan, B., Yang, X. J., Sun, R. Q., Liu, L. Y., Wang, F. Z., & Wang, L. L. (2022) A comparison study of three heating assisted enzyme inactivation pretreatments on the physicochemical properties and edible quality of highland barley grain and flour. J. Cereal Sc 104: 103404. https://doi.org/10.1016/j.jcs.2021.103404
21. Wang, Q., Liu, L. C., Huang, Z. H., Bao, K., Jing, Z. H., & Wu, Q. N. (2023) Structure and physicochemical properties of low digestible Euryale ferox Salisb. seed starch. J. Sci. Food Agric. 103(8): 3850-3859. https://doi.org/10.1002/jsfa.12299
22. Jiang, Y. (2013) Effects of Amino Acids and Fatty Acids on Rice Starch Properties: Thermal, Pasting, Resistant Starch and Structural Characterization. Dissertation, Louisiana State University.
23. BeMiller, J. N., & Whistler, R. L. (Eds.) (1996) Starch: Chemistry and Technology. San Diego, Academic Press.
24. Liu, M. Y., Guo, X. X., Ma, X. Y., Xie, Z. R., Wu, Y. W., & Ouyang, J. (2024) Physicochemical properties of a novel chestnut porous starch nanoparticle. Int. J. Biol. Macromol. 261: 129920. https://doi.org/10.1016/j.ijbiomac.2024.129920
25. Barichello, V., Yada, R. Y., Coffin, R. H., & Stanley, D. W. (1990) Low temperature sweetening in susceptible and resistant potatoes: starch structure and composition. J. Food Sci. 55(4): 1054–1059.
26. Zhou, Y. L., Cui, L. H., You, X. Y., Jiang, Z. H., Qu, W. H., Liu, P. D., Ma, D. Y., & Cui, Y. Y. (2021) Effects of repeated and continuous dry heat treatments on the physicochemical and structural properties of quinoa starch. Food Hydrocolloids 113: 106532. https://doi.org/10.1016/j.foodhyd.2020.106532
27. Cooke, D., & Gidley, M. J. (1992) Loss of crystalline and molecular order during starch gelatinization: origin of the enthalpic transition. Carbohydrate Research 227: 103–112. https://doi.org/10.1016/0008-6215(92)85063-6
28. Singh, N., & Kaur, L. (2004) Morphological, thermal, rheological and retrogradation properties of potato starch fractions varying in granule size. J. Sci. Food Agric., 84(10): 1241-1252. https://doi.org/10.1002/jsfa.1746
29. Ao, Z. C. (2022) [Study on the structural changes of starch granules during grain filling and seed germination of *coix* seed] (Master's thesis). Guizhou University. Available from CNKI China Master's Theses Full-text Database.
30. Binazir, E., Ghanbarzadeh, B., Hanifian, S., Gharekhani, M., Kafil, H. S., & Falcone, P. M. (2024) Development and optimization of thyme-pennyroyal essential oils based active nanostructured lipid carrier (NLC) containing saffron extract with antioxidant and antimicrobial properties. Food Biosci 61: 104992. https://doi.org/10.1016/j.fbio.2024.104992
31. Bajer, D., Kaczmarek, H., & Bajer, K. (2013) The structure and properties of different types of starch exposed to UV radiation: A comparative study. Carbohydr. Polym., 98(1): 477-482.

https://doi.org/10.1016/j.carbpol.2013.05.090

32. Zhang, K. X., Zhang, Z. H., Zhao, M., Milosavljevic, V., Cullen, P. J., Scally, L., Sun, D. W., & Tiwari, B. K. (2022) Low-pressure plasma modification of the rheological properties of tapioca starch. Food Hydrocolloids 125: 107380. https://doi.org/10.1016/j.foodhyd.2021.107380
33. Qiu, S., Yadav, M. P., Chen, H., Liu, Y., Tatsumi, E., & Yin, L. J. (2015) Effects of corn fiber gum (CFG) on the pasting and thermal behaviors of maize starch. Carbohydr. Polym. 115: 246-252. https://doi.org/10.1016/j.carbpol.2014.08.071
34. Brennan, C. S., & Cleary, L. J. (2005) The potential use of cereal (1→3,1→4)-β-D-glucans as functional food ingredients [Review]. J. Cereal Sc, 42(1), 1-13. https://doi.org/10.1016/j.jcs.2005.01.002
35. Zhao, Q., Jiang, L. X., Lian, Z., Khoshdel, E., Schumm, S., Huang, J. B., & Zhang, Q. Q. (2019) High internal phase water-in-oil emulsions stabilized by food-grade starch. J. Colloid Interface Sci *534*: 542-548. https://doi.org/10.1016/j.jcis.2018.09.058
36. Chen, C. J., Li, G. T., & Zhu, F. (2021) A novel starch from lotus (Nelumbo nucifera) seeds: Composition, structure, properties and modifications[Review].Food Hydrocolloids 120: 106899.https://doi.org/10.1016/j.foodhyd.2021.106899

Figures

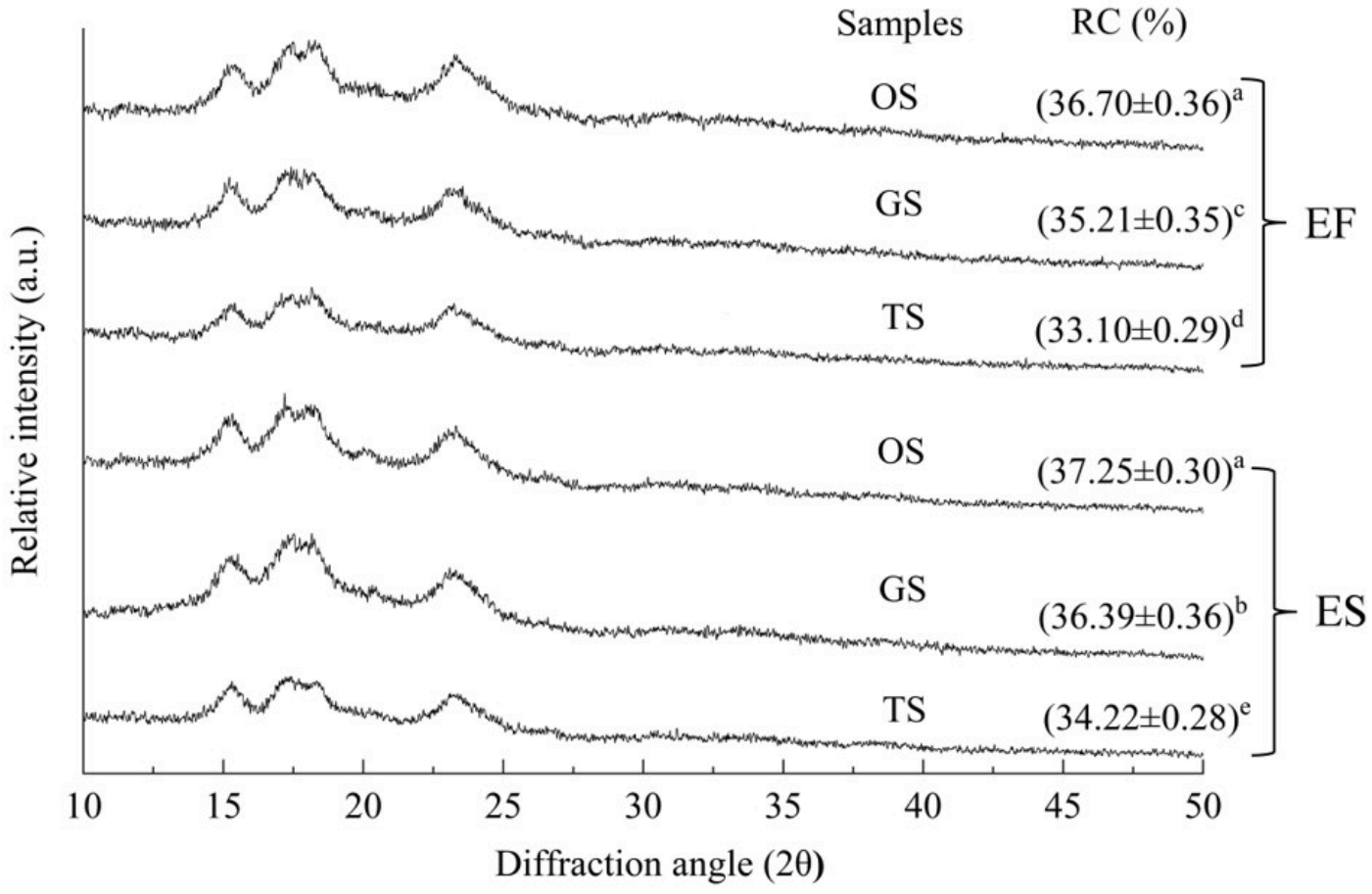


Figure 1

XRD diffraction pattern of thickened powder and starch with different maturity. EF *Euryale ferox* flour, ES *Euryale ferox*starch, TS tender seeds, GS green seeds, OS old seeds, RC relative crystallinity. The different lowercase letters after the RC results in the figure indicate a significant difference between samples ($p < 0.05$).

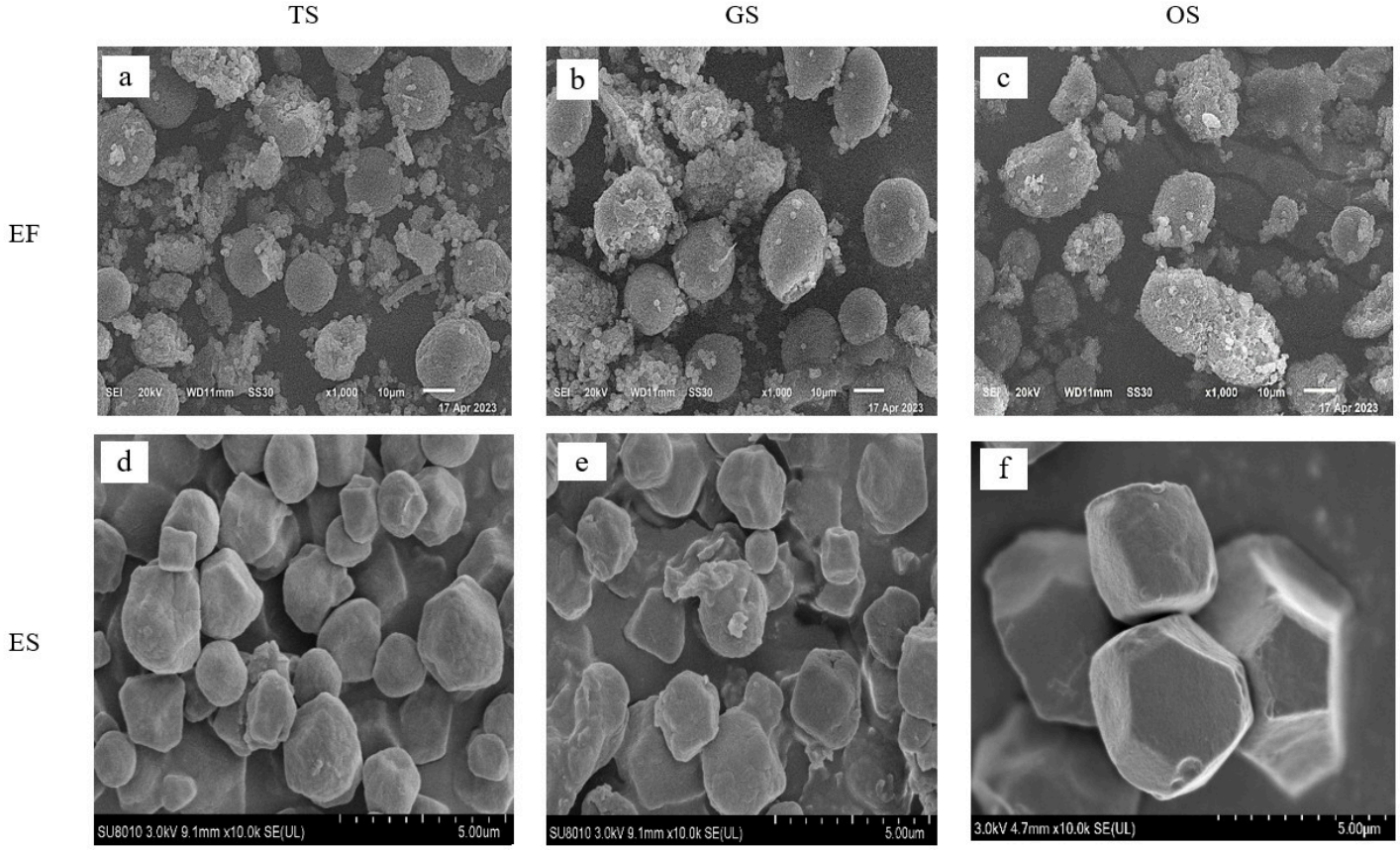


Figure 2

SEM pictures of EF and ES with different maturity. The magnification of the starch is 1000 times, and the magnification of the starch is 10000 times. EF *Euryale ferox* flour, ES *Euryale ferox* starch, TS tender seeds, GS green seeds, OS old seeds

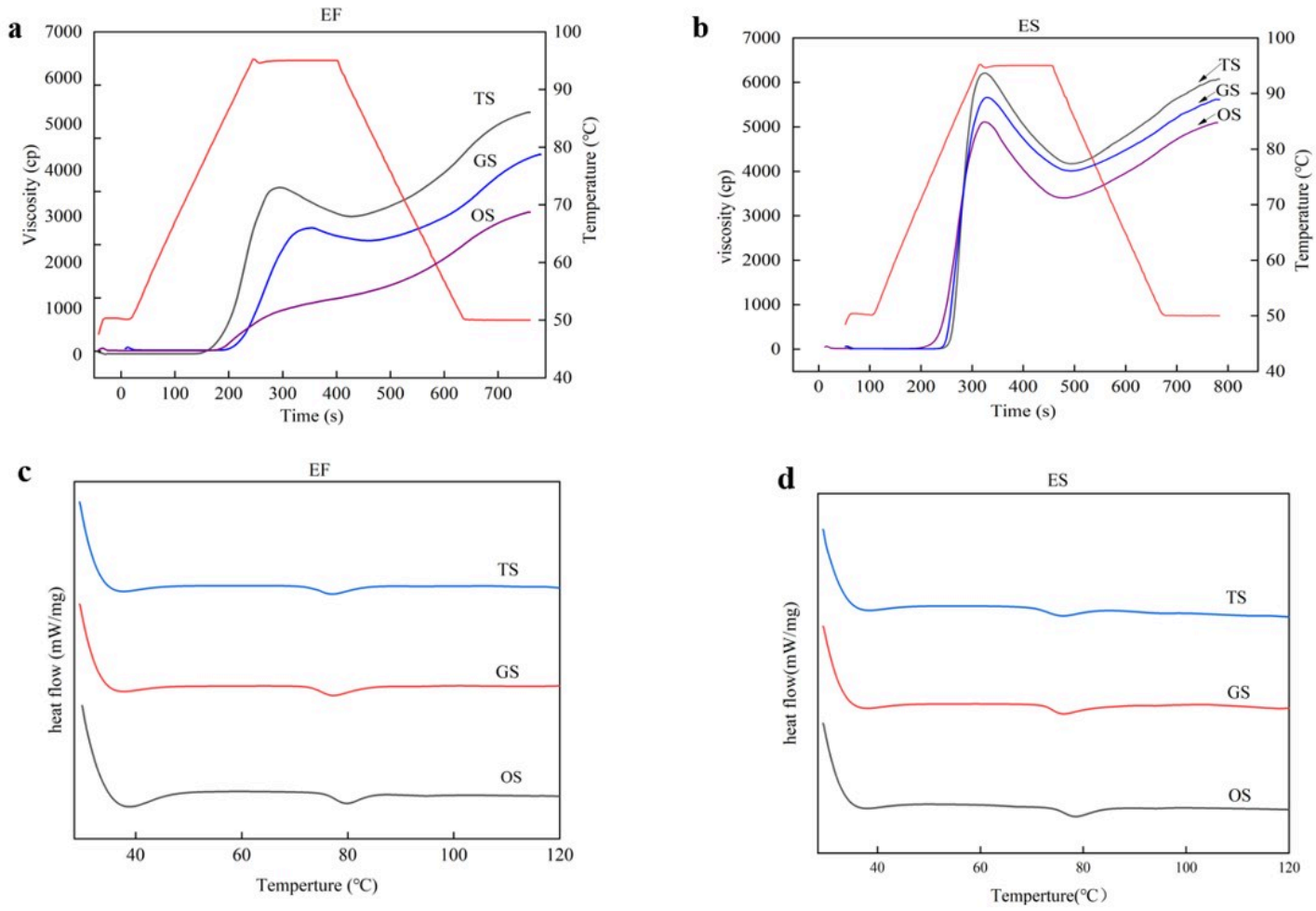


Figure 3

RVA curves (a, b) and DSC curves (c, d) of EF and ES at different maturity levels.EF *Euryale ferox* flour, ES *Euryale ferox* starch, TS tender seeds, GS green seeds, OS old seeds

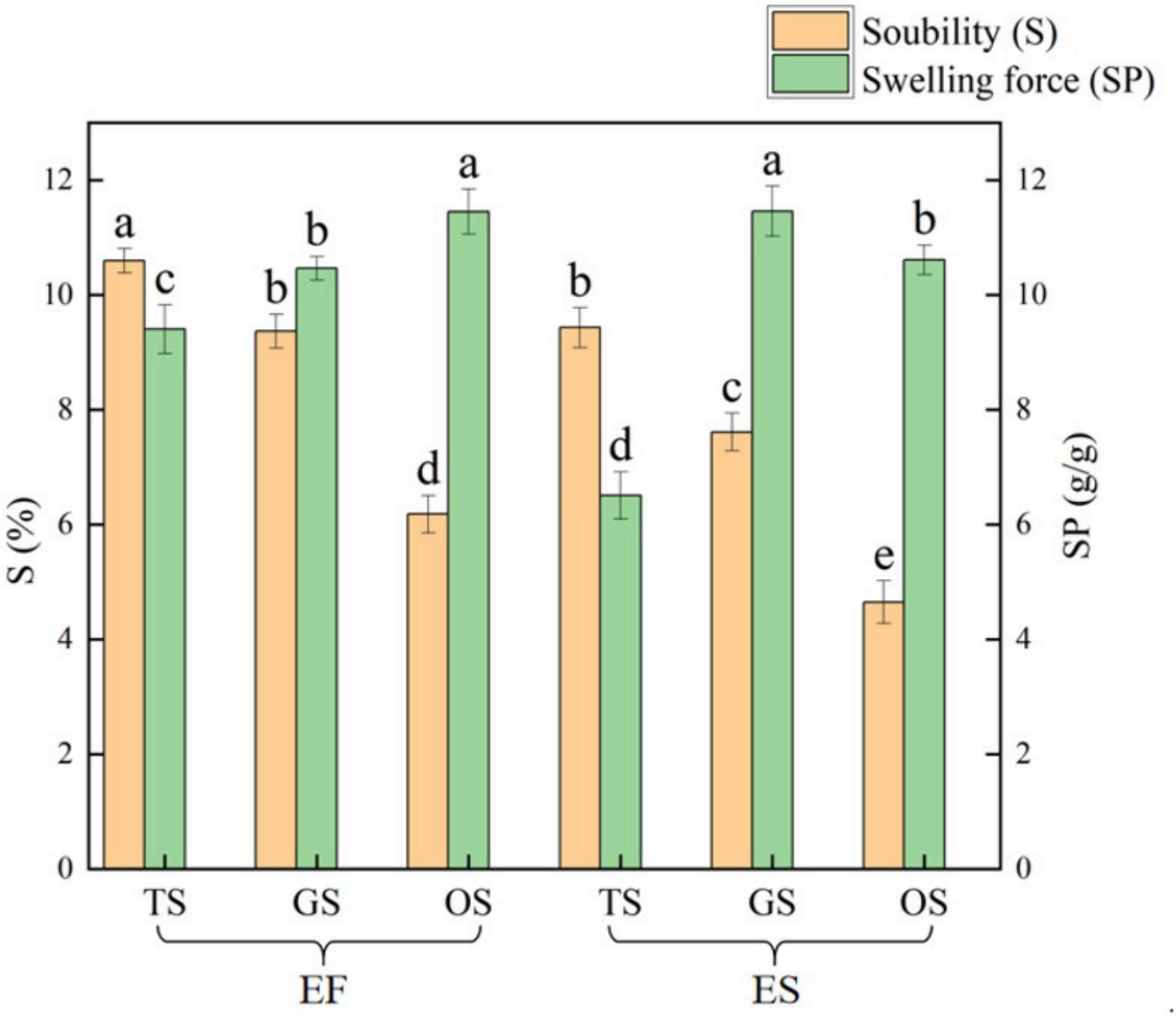


Figure 4

Solubility (S) and swelling power (SP) of EF and ES. EF *Euryale ferox* flour, ES *Euryale ferox* starch, TS tender seeds, GS green seeds, OS old seeds. Different letters in the same series indicate significant differences between them ($p < 0.05$).

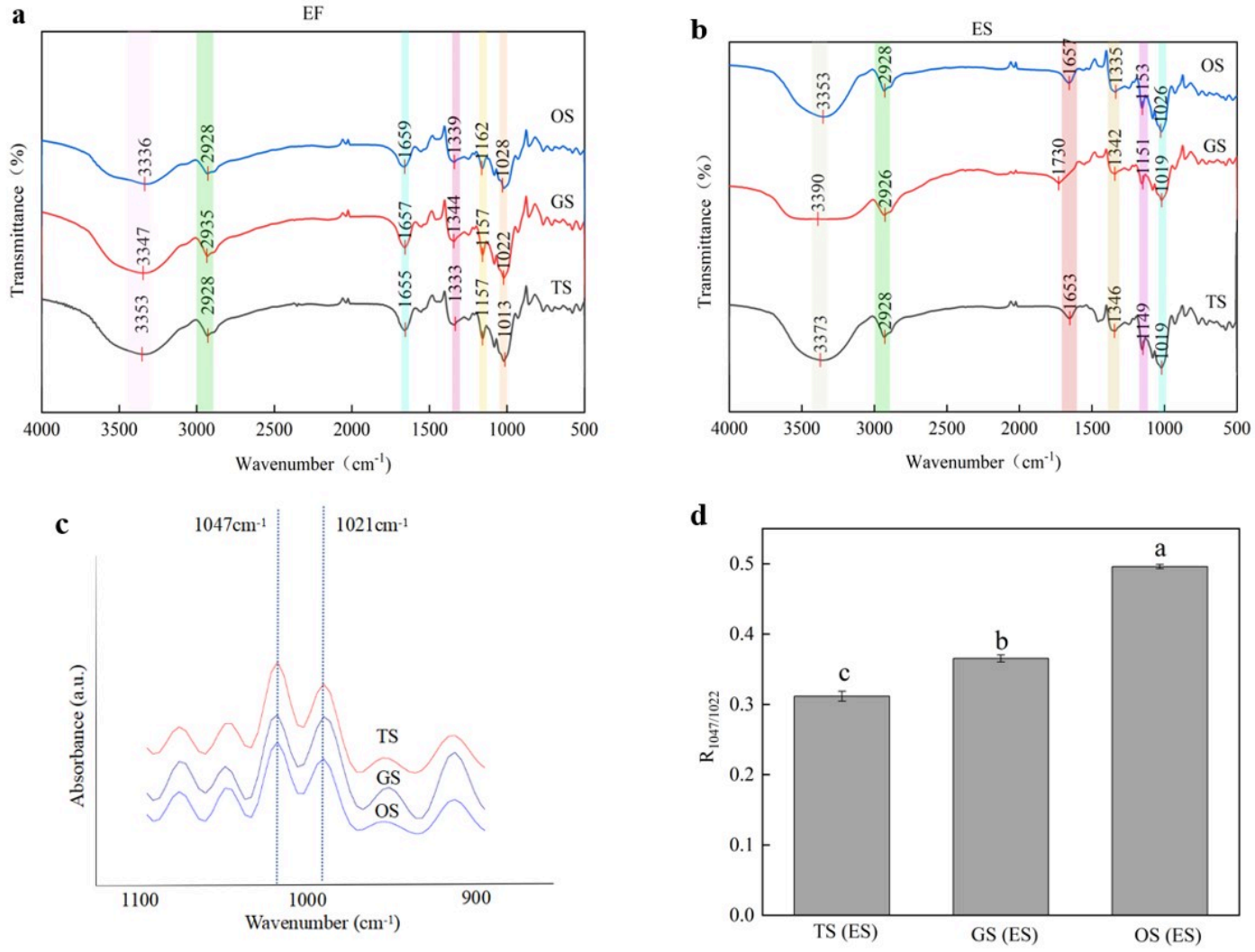


Figure 5

Different maturity of EF (a) and ES FTIR spectrum (b), Deconvolution spectrum of ES (c) and Peak intensity ratio of ES (d). EF *Euryale ferox*flour, ES *Euryale ferox* starch, TS tender seeds, GS green seeds, OS old seeds

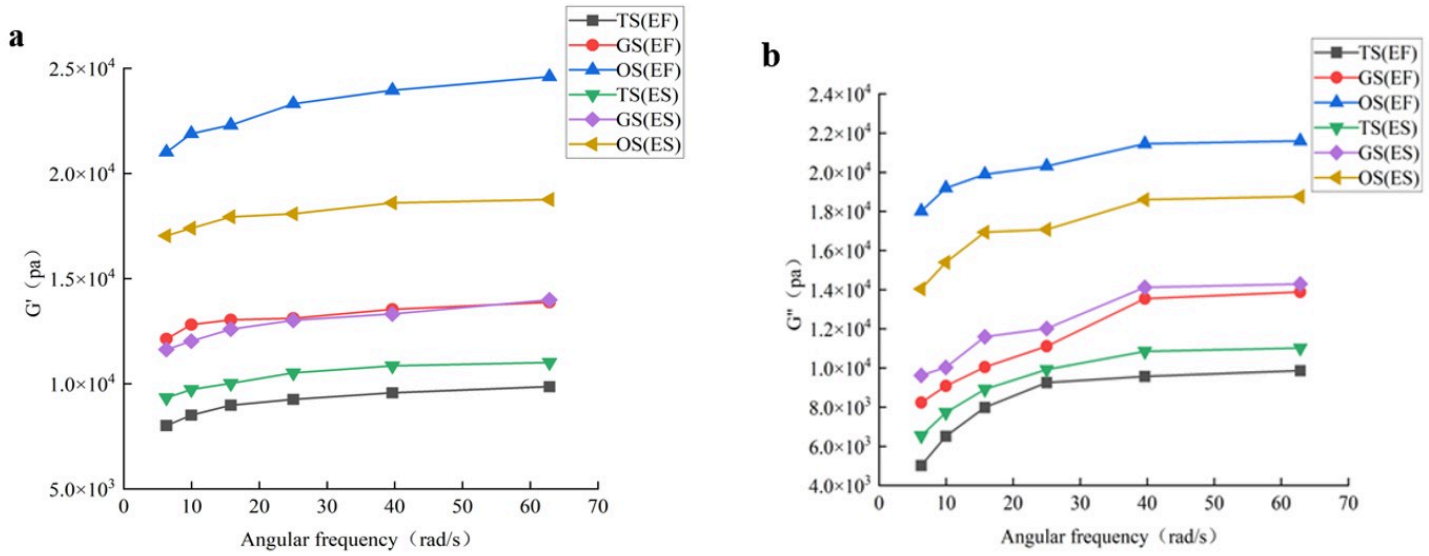


Figure 6

G' (a) and G" (b) of EF and ES samples at vary maturity stages. EF *Euryale ferox* flour, ES *Euryale ferox* starch, TS tender seeds, GS green seeds, OS old seeds

Supplementary Files

This is a list of supplementary files associated with this preprint. Click to download.

- fig.2a.png
- fig.2b.png
- fig.2c.png
- fig.2d.png
- fig.2e.png
- fig.2f.png